Sound & Vibration 2025, 59(4), 3523.
https://doi.org/10.59400/sv3523

Article

Multi-dimensional evaluation and prediction of vibration comfort in electric loaders using ACO-Transformer

Ruxue Dai[1], Jian Zhao[2], Qingli Sui[2], Weidong Zhao[2], Weiping Ding[1], Haibo Huang[1,*]

[1] School of Mechanical Engineering, Southwest Jiaotong University, Chengdu 610031, China
[2] LiuGong Global R&D Center, Liuzhou Liugong Excavator Co., Ltd., Liuzhou 545027, China
*** Corresponding author:** Haibo Huang, huanghaibo214@foxmail.cn

CITATION

Dai R, Zhao J, Sui Q, et al. Multi-dimensional evaluation and prediction of vibration comfort in electric loaders using ACO-Transformer. Sound & Vibration. 2025; 59(4): 3523. https://doi.org/10.59400/sv3523

ARTICLE INFO

Received: 14 July 2025
Revised: 1 August 2025
Accepted: 28 August 2025
Available online: 29 August 2025

Abstract: Engineering machinery plays a vital role in supporting modern economic development. The electric loader represents a key innovation driven by environmental protection and the pursuit of sustainable development. However, the absence of engine masking effects in electric machinery makes structural vibration and impact noise more pronounced. To address this issue, this study proposes an ant colony optimization-Transformer (ACO-Transformer) model that integrates the ant colony algorithm with the Transformer framework to accurately and efficiently evaluate the vibration comfort of electric engineering machinery. An improved objective evaluation method for vibration was employed to extract objective data from four measurement points, while 34 subjective scores were obtained through a structured subjective evaluation protocol. The combined analysis of subjective and objective data demonstrated the validity of incorporating additional vibration measurement points. Using these datasets, the ACO-Transformer model was developed to establish a mapping between multi-dimensional objective vibration parameters and subjective comfort ratings. Results indicate that the proposed model achieved high prediction accuracy (MAPE = 6.22%) and strong generalization performance (RMSE = 6.11). This study offers a novel approach for evaluating and predicting the vibration comfort of engineering machinery cabins.

Keywords: ACO-Transformer; operator comfort; vibration prediction

1. Introduction

With the increasingly prominent problem of global warming, the development of green and clean energy has become an important strategy for the development of modern industry [1]. Driven by the new round of product technology change and the trend of energy conservation and emission reduction, electrification has gradually become the preferred solution for the global engineering machinery industry to cope with energy shortage and reduce environmental pollution [2]. Compared with traditional engineering machinery, electric engineering machinery lacks the masking effect of engine noise, which makes the vibration and impact noise of other structures more significant [3]. This has brought new challenges to the Noise, Vibration and Harshness (NVH) performance research of engineering machinery, and has also caused great obstacles to the further improvement of the NVH performance of electric engineering machinery.

In addition, under the background of the rapid development of modern engineering technology, engineering machinery is gradually developing in the direction of large-scale and complicated, which also leads to the increasingly obvious vibration problem in the cab of engineering machinery [4]. Drivers are in a harsh environment with strong vibration for a long time, which is prone to physical fatigue

and obvious discomfort. Long-term accumulation will even reduce the driver's alertness and response ability to emergencies [5]. This will not only seriously affect the driver's work efficiency, but also adversely affect the safety of the working process and the stable operation of the equipment [6]. Globally, the vibration comfort of engineering machinery has become an important indicator to measure the quality of its products [7]. Establishing an objective and accurate evaluation method of vibration comfort in the cab of engineering machinery can not only guide R & D personnel to better improve the system design, but also reduce the driver's discomfort response, thereby significantly improving user satisfaction and enhancing the market competitiveness of products [8,9]. Therefore, it has become an important research direction to propose an efficient and reliable evaluation method for vibration comfort of engineering machinery cab.

1.1. Research status of vibration comfort evaluation

Comfort evaluation is an important way to reflect the ride comfort performance. Comfort evaluation mainly includes subjective evaluation and objective evaluation [10]. Subjective evaluation belongs to the traditional and most effective comfort evaluation method [11]. Commonly used subjective evaluation methods include: simple ranking method [12], numerical estimation method [13], ranking scale method [14], paired comparison method [15], semantic segmentation method, etc. [16,17]. Xiong et al. [18] proposed a quantitative analysis and evaluation method based on the subjective scoring method of NVH characteristics, and obtained the vibration variation law of the three models at different mileage stages. Ao et al. [19] concluded that seat surface vibration contributes the most to comfort by analyzing the subjective evaluation results of vehicle dynamic comfort. Based on the road test, Wu et al. [20] formed an evaluation method to evaluate the seat vibration comfort in a wide range of backrest angles. The results show that under certain conditions, the subjective perception of occupant vibration comfort will deteriorate with the increase of vehicle speed or backrest tilt. To obtain accurate and reliable subjective evaluation results, subjective evaluation methods usually need to be flexibly adjusted according to the test model [21–23]. Although some subjective evaluation studies on vibration comfort have been carried out in the field of engineering machinery, the research on the subjective evaluation of vibration comfort of electric loaders is mainly based on the field of automobiles, which makes the previous subjective evaluation methods of vibration comfort often show some limitations in practical applications [24]. Therefore, combined with engineering practice, this study proposes a subjective evaluation method that combines semantic segmentation method and ranking scale method, and subjectively evaluates the vibration measuring points studied respectively to comprehensively evaluate the vibration comfort of the loader cab.

Objective evaluation the dynamic characteristics of vibration are objectively quantified by measuring instruments, and objective parameters are formed to evaluate the advantages and disadvantages of vibration comfort [25–27]. At present, the objective evaluation of vibration comfort is mainly based on ISO-2631 [28], BS-6841 [29] and VDI-2057 [30]. Based on ISO-2631, Ciloglu et al. [31] evaluated the vibration comfort of each position in the aircraft cabin and gave suggestions for improvement. Carletti et al. [32] made an objective evaluation of the vibration comfort of the loader seat, and the

results showed that the comfort of the seat in the horizontal direction was inferior to that in the vertical direction. The existing research standards usually only evaluate the vibration comfort of the seat. Zhao et al. [33] found that the driver's comfort requirements for the cab will change over time, and a single seat vibration comfort cannot represent the vibration comfort of the loader cab. Therefore, researchers improved and optimized the objective evaluation method by introducing additional measuring points [34]. Zhao et al. [35] added pedal and joystick measuring points to comprehensively evaluate the vibration comfort of the harvester. The results show that the vibration at the pedal is stronger than other measuring points, which is the main factor affecting the comfort. Considering the objective fact that the loader driver's arm is often touched or placed on the seat, this study adds the measuring point at the armrest based on the traditional three measuring points, and further improves the objective evaluation method of vibration comfort. Considering the symmetry and functional consistency of the left and right armrest structures, an objective evaluation method of vibration comfort at four measuring points including floor, seat, back and left armrest was finally formed.

The subjective evaluation method and the objective evaluation method have their own inherent shortcomings and limitations in practical engineering applications [36]. At the same time, considering the rapid development of machine learning, researchers began to use the subjective and objective mapping model to study the vibration comfort of the cab, aiming at considering the advantages of subjective and objective evaluation [37]. Since simple linear mapping cannot represent the nonlinear relationship between subjectivity and objectivity [38–40], researchers have introduced machine learning models to establish a nonlinear mapping from objective vibration indicators to subjective human perception. Huang et al. [41] used the neural network model to establish the mapping relationship between the dynamic objective parameters of the vehicle cab and the subjective comfort. Du et al. [42] developed a new method for evaluating vehicle vibration comfort based on frequency domain vibration signals using deep learning. Nevertheless, the traditional machine learning model often shows insufficient ability to deal with the multi-input and multi-output problems in the process of subjective and objective mapping, and it is difficult to fully explore the deep correlation between the information of each vibration dimension. Based on this, this study proposes an ACO-Transformer, which is used to construct a nonlinear mapping relationship between subjective and objective evaluation of vibration comfort of loader cab.

1.2. Analysis of related works

In summary, there are still many deficiencies in the current research on the evaluation and prediction of vibration comfort of electric loader cabs. In terms of subjective evaluation, the current subjective evaluation methods are directly derived from the automotive field, and usually use a single score to characterize the overall comfort level. A single score lacks a detailed description of the vibration comfort performance of each part of the cab. In terms of objective evaluation, the existing objective evaluation methods are still based on the traditional three measuring points, mainly for the evaluation of seat comfort, and fail to fully consider the vibration

comfort of the loader cab. Regarding the construction of the subjective and objective mapping model of the vibration comfort of the loader cab, there is currently no subjective and objective mapping model suitable for multi-dimensional vibration objective parameter input and multi-dimensional vibration comfort subjective score output.

The main contributions of this paper as follows:

1) To comprehensively evaluate the vibration comfort in the loader cab, this paper evaluates the main contact parts of the driver and seat, floor, back and armrest based on the improved subjective evaluation method, and systematically describes the vibration comfort of the cab from four dimensions.

2) Combined with the driver's contact attitude and vibration transmission path in the actual operation process, this paper introduces the left armrest as a new measuring point based on the traditional three measuring points, and constructs a four-point vibration comfort objective evaluation method for electric loaders.

3) In this paper, a Transformer model based on ant colony optimization algorithm is proposed to accurately complete the establishment of a loader vibration comfort prediction model with multi-input of objective vibration indicators and multi-output of subjective evaluation.

The structure of the article: 1) Section2 briefly describes the Transformer model and proposes an improved ACO-Transformer algorithm. 2) Section3 introduces the subjective and objective test method of vibration comfort of loader cab and the corresponding test process. 3) Section4 analyzes the subjective and objective test results, and analyzes the proposed host-guest results. 4) Section5 Based on the ACO-Transformer method, the vibration comfort prediction model of loader cab is established, and the correlation analysis of the prediction results is carried out. 5) Section6 summarizes the full text based on the research content.

2. Research methods

2.1. A brief introduction of transformer

Transformer was originally proposed by Vaswani et al. in 2017. All the calculation processes rely on the attention mechanism, completely abandon the loop and convolution structure, and have good parallel computing ability and long-distance dependence modeling ability. Transformer has become one of the basic model architectures in multi-objective learning tasks [43]. Transformer is a deep learning model based on attention mechanism. The multi-head attention mechanism characterizes and weights the input information from different angles through parallel multiple attention sub-modules, thereby improving the model's perception of contextual features and expression diversity [44]. The specific structure of the multi-head attention mechanism is shown in **Figure 1**.

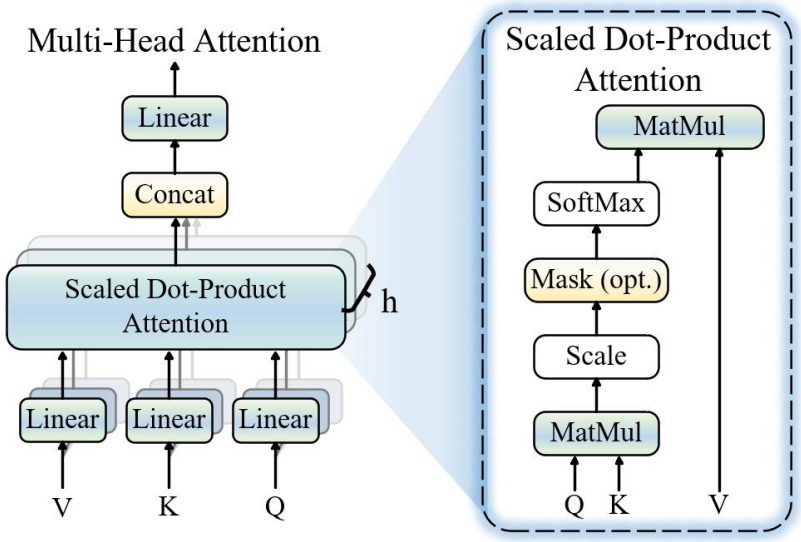

Figure 1. Multi-head attention.

The single-head attention mechanism generates a query matrix *Q*, a key matrix *K*, and a value matrix *V* by performing three linear transformations on the vectors at each position in the input sequence. Its calculation equation is Equation (1):

$$Attention(Q,K,V) = softmax(\frac{QK^T}{\sqrt{d_k}})V \tag{1}$$

where, *Q*, *K* and *V* represent Query, Key and Value matrices respectively, and d_k is the dimension of the key vector, which is used to scale the dot product to stabilize the softmax function.

In multi-head attention, this mechanism will perform *h* times in parallel to form *h* attention heads, and each head uses an independent linear transformation matrix to map the input to different subspaces. And perform self-attention calculation independently in each subspace. Specifically, as shown in Equation (2):

$$head_i = Attention(QW_i^Q, KW_i^K, VW_i^V) \tag{2}$$

where, W_i^Q, W_i^K, $W_i^V \in R^{d\times d_k}$ is the linear transformation matrix of the first *i*-head.

After completing the self-attention operation of all heads, the output results will be spliced and fused through a unified linear transformation to integrate information from multiple subspaces, and finally output the results of multi-head attention, as shown in Equation (3):

$$MultiHead(Q,K,V) = Concat(head_1,\ldots,head_H)W^O \tag{3}$$

where, $W^O \in R^{Hd_v\times d_o}$ is the weight matrix of the output layer, and *Concat* represents the splicing operation.

The Transformer model is mainly composed of four parts: input, encoder, decoder and output. Usually, the encoder and decoder stacks have 6 layers, each layer contains multi-head self-attention, feedforward network, residual connection and layer norm.

The specific structure of Transformer is shown in **Figure 2**. The overall operation process of the Transformer model is as follows: First, the input sequence is added to the position encoding through the word embedding layer and converted into a vector representation with sequential information and sent to the encoder part. The encoder is stacked by multiple sub-layers with the same structure. Each sub-layer contains a multi-head attention mechanism and a feedforward neural network. The training stability and expression ability of the model are improved by residual connection and layer normalization. The output of the encoder captures the global dependencies between the feature positions in the input sequence, forming a set of context-dependent high-dimensional representations.

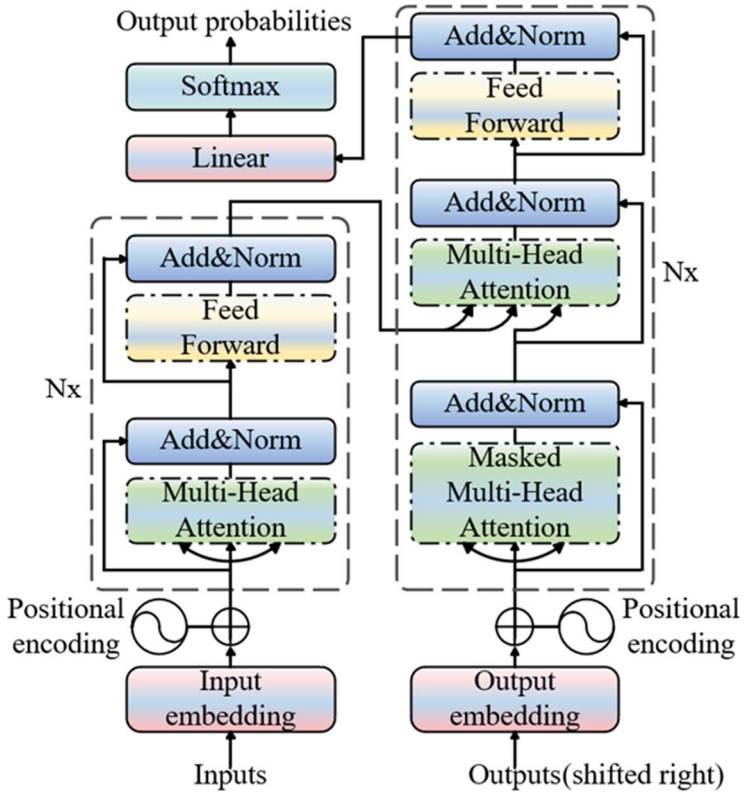

Figure 2. Transformer structure diagram.

Subsequently, the decoder gradually generates the target sequence, whose structure is like that of the encoder, but a masking self-attention mechanism is added in each layer to prevent information leakage, and the encoder-decoder attention module enables the decoder to focus on the key information of the input sequence. The decoder receives the predicted completed part as input and performs context modeling with the output representation of the encoder. Finally, the decoder output obtains the probability distribution of each predicted target at each output position through a linear transformation layer and a *Softmax* function, thereby gradually generating a complete output sequence.

2.2. ACO-Transformer

Ant Colony Optimization (ACO) algorithm is a swarm intelligence optimization method inspired by the foraging behavior of ants in nature [45,46]. The algorithm

forms a random optimization strategy based on positive feedback and parallel search by simulating the mechanism of ants relying on pheromones for collaborative search in the process of finding food [47]. In the early stage of the algorithm, a certain number of "artificial ants" randomly select paths in the solution space to construct feasible solutions. The quality of each path is determined by the objective function value and is indirectly expressed by the pheromone concentration [48,49]. The core idea of the ant colony optimization algorithm is that the denser the pheromone on the path, the greater the probability that the subsequent ants choose the path, to strengthen the pheromone accumulation of the high-quality path in the continuous iteration and realize the gradual approximation of the global optimal solution. The whole process includes path construction, pheromone update, heuristic function guidance and other operations. Through information sharing and distributed collaboration between individuals, the quality of the solution is gradually optimized. The ant colony optimization algorithm makes full use of the dynamic balance mechanism of local exploration and global guidance, and has strong robustness and parallelism. It is widely used in complex search tasks such as combinatorial optimization, path planning and scheduling problems.

Several key hyperparameters (such as the number of encoder layers and the number of attention heads) in the Transformer model will significantly affect the convergence speed, prediction performance and generalization ability of the model on different tasks. If these parameters can be jointly optimized, it will help to achieve a better balance between modeling accuracy, computational efficiency and model complexity. The traditional grid search method is inefficient in high-dimensional parameter space, and the search process is easy to fall into local optimum, which is difficult to meet the parameter adjustment requirements of complex models. In contrast, the ant colony optimization algorithm, as a global optimization strategy that simulates the foraging behavior of ant groups, has significant advantages in search speed and global exploration ability. Therefore, this study introduces ACO to optimize the key hyper-parameter combination of Transformer model.

This process first initializes a group of "ants" in a predefined parameter space, each ant represents a parameter combination path, and learns the training data by constructing a Transformer model, and then calculates the fitness value of the path according to the prediction accuracy of the model on the verification set (the update basis of pheromone concentration). In each iteration, the ants jointly determine the selection direction of the next parameter according to the pheromone concentration and the heuristic function, and release new pheromones on all paths to enhance the search probability of the high-quality parameter combination. By continuously repeating the path construction, pheromone update and iterative optimization process, the algorithm can efficiently search and approximate the optimal parameter configuration of Transformer in the high-dimensional complex parameter space. The overall process of optimizing Transformer hyperparameters by ant colony optimization algorithm is shown in **Figure 3**.

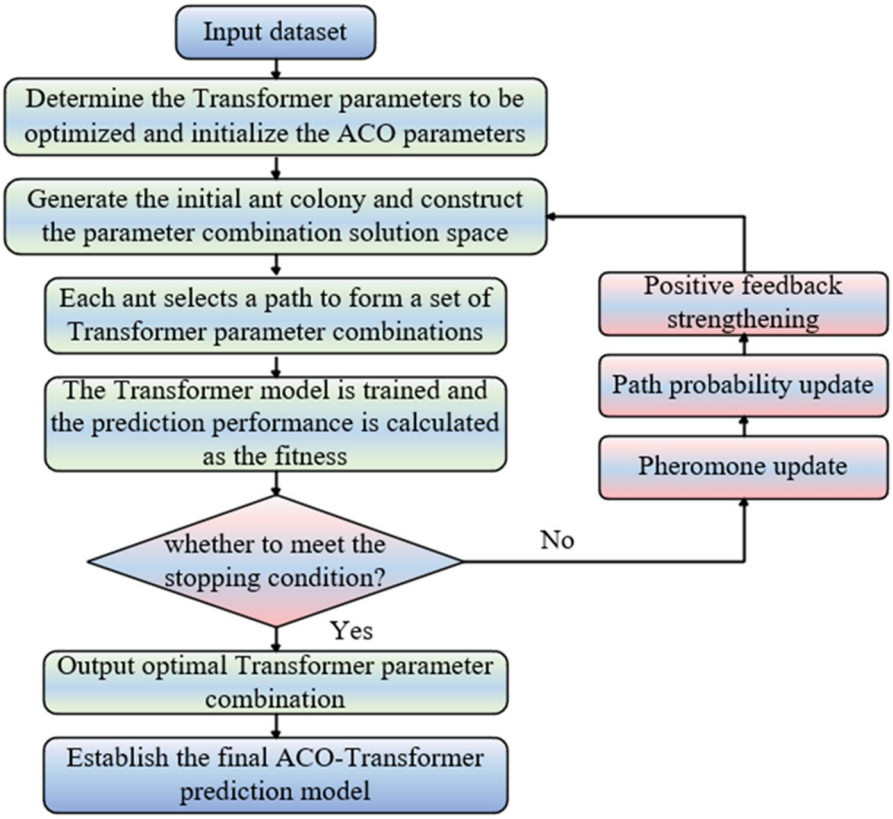

Figure 3. ACO-Transformer structure diagram.

3. Vibration comfort subjective and objective test of loader

3.1. Subjective test of vibration comfort

In this study, a subjective evaluation method for vibration comfort of loader cab is constructed by combining semantic segmentation method and ranking scale method to collect driver's subjective score. This study first uses the semantic segmentation method to divide the perception range of vibration into five levels to ensure that the scoring system has sufficient resolution, while avoiding the driver's cognitive burden caused by too many levels [50]. Considering the high vibration level of the loader under normal working conditions, the third level is defined as a neutral level to adapt to its use environment. In addition, to reduce the experience dependence of evaluators, this study has carried out specific language descriptions for each level. On this basis, the ranking scale method is introduced, and each level is divided into two subdivision scoring intervals, so that the subjective score falls into the range of 1 to 10, and finally a subjective scoring standard of 10 grades is formed.

In addition, in the subjective evaluation of the vibration comfort of the loader, considering that the driver's arm often touches or is placed on the armrest, as well as the symmetry and functional consistency of the left and right armrests in the structure, this paper adds the left armrest measuring point on the basis of the traditional three measuring points of the seat, floor and back, and scores the four measuring points separately in the subjective evaluation, so as to realize the comprehensive evaluation of the vibration comfort of the cab. In this study, a subjective evaluation table of vibration comfort was formed by combining the subjective evaluation method of

comfort and the specific perceived parts of the loader cab, as shown in **Table 1**.

Table 1. Loader vibration comfort subjective rating scale.

Name:	**Driving age:**	**Sex:**	**Date:**		
Score	**Evaluation level**	**Detailed descriptions**	**Evaluation score**		
1 2	Poorly feel	Strong sense of shock at the contact area	Point	Lifting	Lowering
3 4	Uncomfortable	The contact area feels numb	Back		
5 6	Neutral	The contact area feels slightly numb	L-armrest		
7 8	Feeling slight	No numbness at the contact area	Seat		
9 10	No discomfort	The contact area feels completely normal	Floor		

Notes: L stands for Left, and other locations in the text are similar.

To study the vibration comfort of loaders, this study carried out a subjective evaluation test of comfort based on a 20-ton electric loader of LIUIGONG. The evaluation conditions are two typical working conditions of loader lifting and lowering. For subjective evaluation, a total of 35 loader drivers with 5–20 years of driving experience were recruited in this study. To ensure the accuracy and validity of the evaluation results, all drivers underwent neurological examination and vibration sensitivity assessment before participating in the test [51]. Finally, a total of 34 drivers participated in the subsequent subjective evaluation experiment through screening.

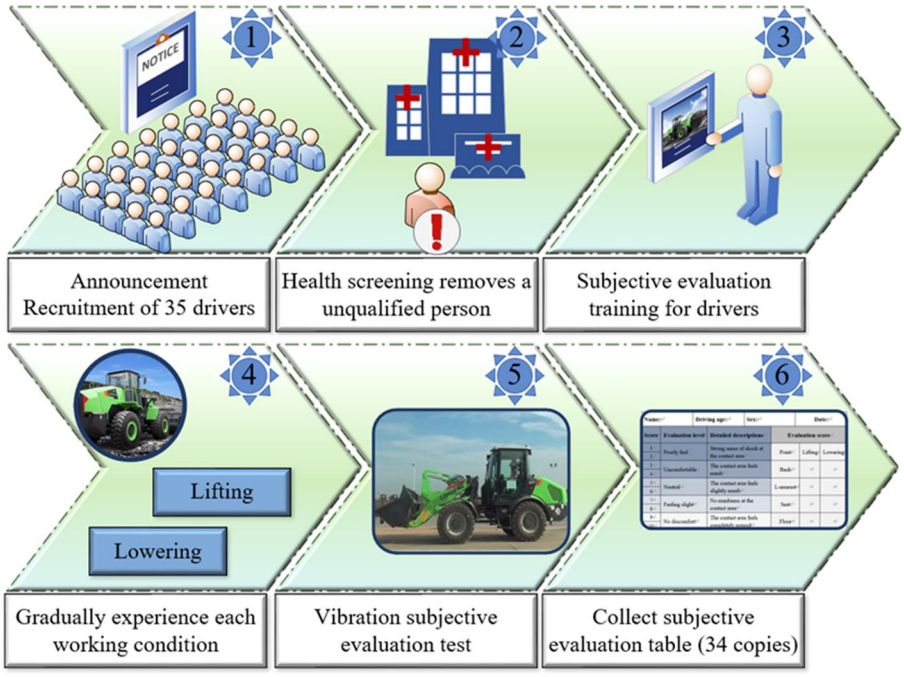

Figure 4. Electric loader subjective evaluation test flow chart.

Before the formal test, this study conducted a unified training for all participants,

and explained in detail the subjective evaluation process, scoring criteria and precautions to ensure that the driver has a clear understanding of the evaluation system and has basic judgment consistency. Then, the driver runs the lifting and lowering conditions one by one, and is familiar with each typical working condition, to have a clear subjective reference scale in the actual scoring process. In the process of formal subjective evaluation, each driver performs lifting and lowering conditions in turn, and the duration of each condition is 3 seconds. After the completion of the operation, the driver independently evaluated the vibration comfort of the four measuring points under the two working conditions according to the subjective scoring criteria given in Table 1. The complete subjective evaluation test process includes a total of 6 links; the specific steps are shown in **Figure 4**.

3.2. Vibration comfort objective test

Considering the objective fact that the driver's arm of the loader often touches or is placed on the seat during operation, this study adds a measuring point at the armrest. In addition, due to the symmetry of the left and right armrest structure and the longer time that the driver's left arm is placed on the armrest, the left armrest is used as a new measuring point. Finally, the objective test scheme of vibration comfort of 4 measuring points is formed as shown in **Figure 5**. Numbers 1 to 4 in the figure correspond to the four measuring points of seat, back, floor, left armrest.

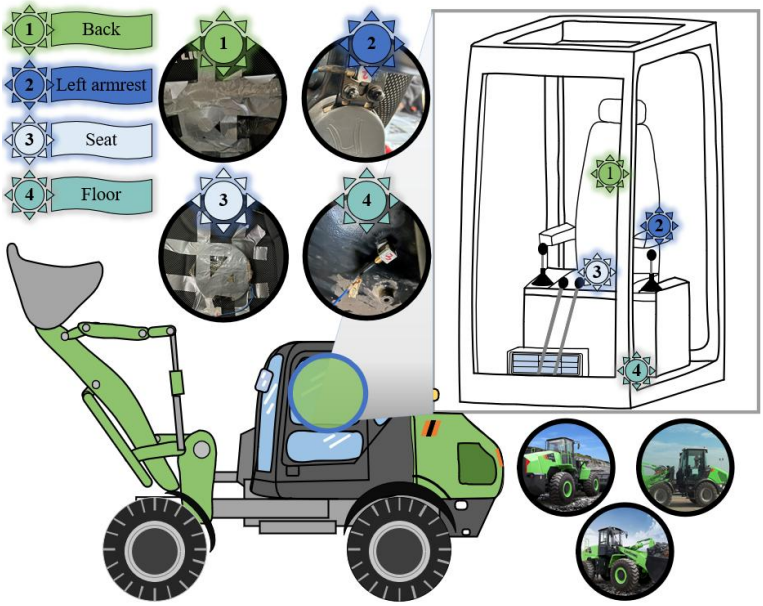

Figure 5. Electric loader real vehicle test point layout.

The objective test is carried out by SIEMENS LMS SCADAS Mobile 16-channel data acquisition system. The sensor model and technical specifications are shown in **Table 2**. To ensure the validity and comparability of the test results, the objective test and the subjective evaluation are carried out simultaneously to ensure that the objective data and the subjective results can be mutually verified, and can support the subsequent subjective and objective data analysis and modeling. Considering that the sensitive frequency band of human body to vibration is mainly 0.5–80 Hz [52], this

study sets the sampling frequency to 512 Hz to ensure that the sampling frequency of the vibration signal meets the resolution requirements and can fully capture the relevant dynamic characteristics. In addition, the sampling time of each working condition (lifting, lowering) is set to 3 seconds.

Table 2. List of test points for actual vehicle testing.

Name	Category	Type
Seat	Vibration acceleration sensor	S01410
Floor	Vibration acceleration sensor	SN-J0810
Back	Vibration acceleration sensor	S01410
L-armrest	Vibration acceleration sensor	SN-J0811

Due to the large number of objective test results, this paper selects the objective data collected by a driver during the operation of lifting conditions and lowering conditions for display. The time domain response of each measuring point is shown in **Figure 6**. The vibration signals of the seat, floor, backrest and left armrest under two typical working conditions are shown in the figure. The results show that the Z-axis vibration of the floor position is more significant, while the vibration in the X-axis direction is more obvious at the seat, back and left armrest. This may be because the bucket mainly moves in the vertical direction during the operation of the loader, and the vertical impact will be transmitted through the path of the tire-frame-floor, resulting in the maximum Z-axis vibration at the floor. The seat system usually can better suppress the Z-axis vibration, but the horizontal vibration suppression effect is relatively weak, resulting in more obvious vibration in the X direction of the seat, back and left armrest. In addition, by comparing the lifting and lowering conditions, it can be found that the vibration amplitude of each measuring point in the lifting process is generally greater than that in the lowering condition. This is because the hydraulic system needs to overcome the gravity to lift the boom and bucket together with the load during the lifting process. The impulse response generated by the hydraulic system will enhance the structural vibration, resulting in greater vibration intensity.

Based on the subjective test and objective test of the vibration comfort of the electric loader, a total of 34 driver's data samples were collected, and each driver operated under two typical working conditions of lifting and lowering respectively, so a total of 68 sets of working condition sample data were obtained.

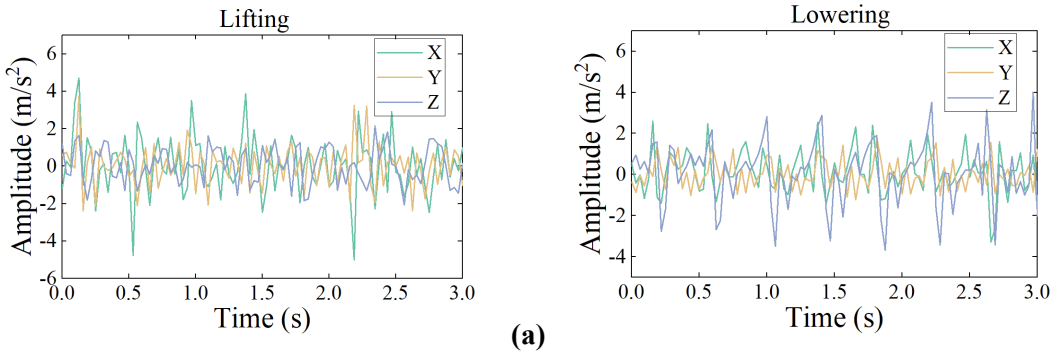

(a)

Figure 6. (*Continued*).

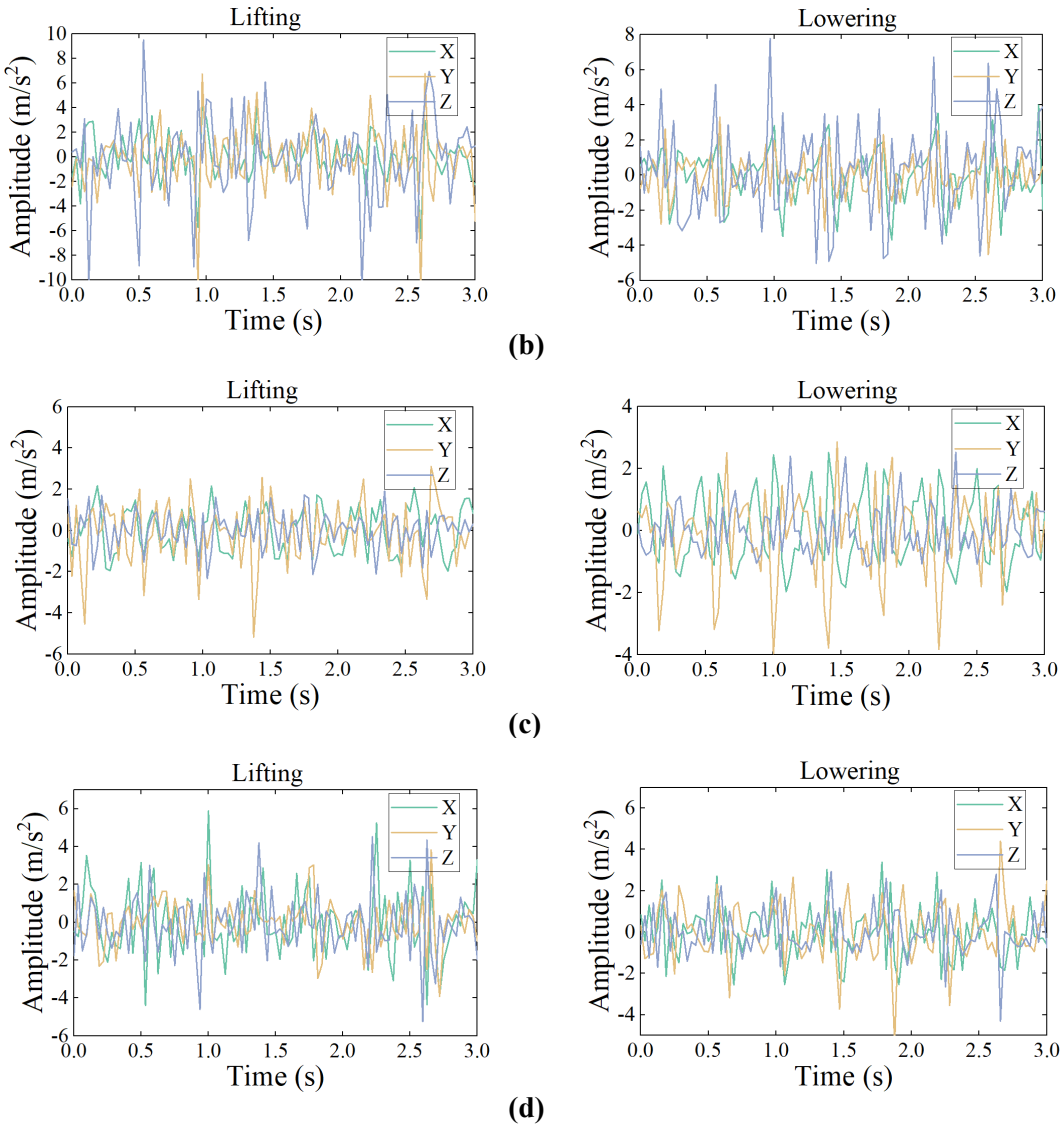

Figure 6. Electric loader each measuring point vibration signal time domain diagram: **(a)** The vibration signal of the seat position under lifting and lowering conditions; **(b)** The vibration signal of the floor position under lifting and lowering conditions; **(c)** The vibration signal of the back position under lifting and lowering conditions; **(d)** The vibration signal of the left armrest position under lifting and lowering conditions.

4. Analysis of subjective and objective test results of loader

4.1. Analysis of subjective test results of vibration comfort

After the completion of the subjective and objective tests, the subjective evaluation results were statistically analyzed, and the scatter plot shown in **Figure 7** was drawn. The analysis results show that the subjective score distribution of each measuring point is relatively close. This may be due to the small difference in the vibration transmission characteristics of the loader cab between different measuring points. This result also shows that the subjective evaluation method proposed in this study can unify the driver's evaluation criteria for different measuring points, thus reducing the discreteness of the scoring results. By further observing the box diagram of each gear, the subjective score is mainly concentrated in the range of 3-10 points,

and there is no extreme negative evaluation below 3 points. This may be because in the process of subjective evaluation, if there is no clear negative guidance, evaluators tend to give more positive feedback and usually do not make too low scores.

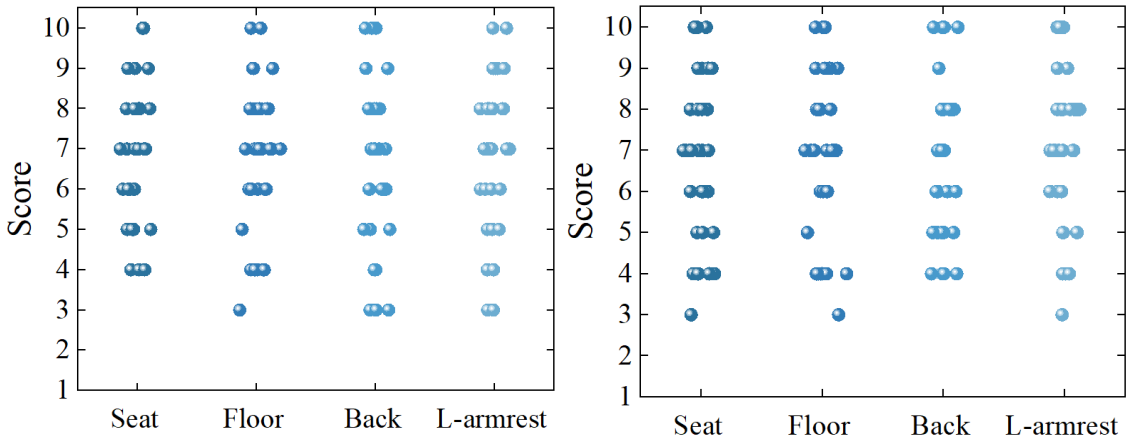

Figure 7. The subjective score distribution of each measuring point in each working condition: **(a)** the subjective score distribution of each measuring point in the lowering condition; **(b)** the subjective score distribution of each measuring point in lifting condition.

To further explore the internal relationship between the comfort evaluation of different vibration measuring points, the correlation analysis was carried out on the subjective scores of the four measuring points of seat, floor, back and left armrest. Pearson correlation coefficient is used to calculate the correlation, and the calculation formula is shown in Equation (4), and the correlation heat map shown in **Figure 8** is drawn. To more intuitively quantify the degree of correlation between the measuring points, this paper further counts all Pearson correlation values, as detailed in Appendix Table A1.

$$\rho_{X,Y} = \frac{Cov(X,Y)}{\sigma_X \cdot \sigma_Y} = \frac{\sum_{i=1}^{n}(x_i - E(X))(y_i - E(Y))}{\sqrt{\sum_{i=1}^{n}(x_i - E(X))^2} \cdot \sqrt{\sum_{i=1}^{n}(y_i - E(Y))^2}} \tag{4}$$

where X and Y are the two variables involved in the calculation, x_i, y_i are the values of variables X and Y in the i th sample, and n is the number of samples.

By analyzing the correlation heat map shown in **Figure 8**, the correlation between the subjective scores of each vibration measuring point is generally high, all of which exceed 0.7. Among them, in the lowering condition, the correlation between the left armrest and the floor is up to 0.9, in the lifting condition, the correlation between the seat and the floor is 0.87. The above results show that there is a significant internal coupling relationship between the vibration evaluation dimensions. Therefore, if only a single dimension score is used as the subjective evaluation result of the vibration comfort of the cab, it may be difficult to fully reflect the vibration characteristics and comfort differences of each part of the cab. To accurately describe the overall comfort level of the cab, it is necessary to construct an evaluation method containing multiple evaluation dimensions.

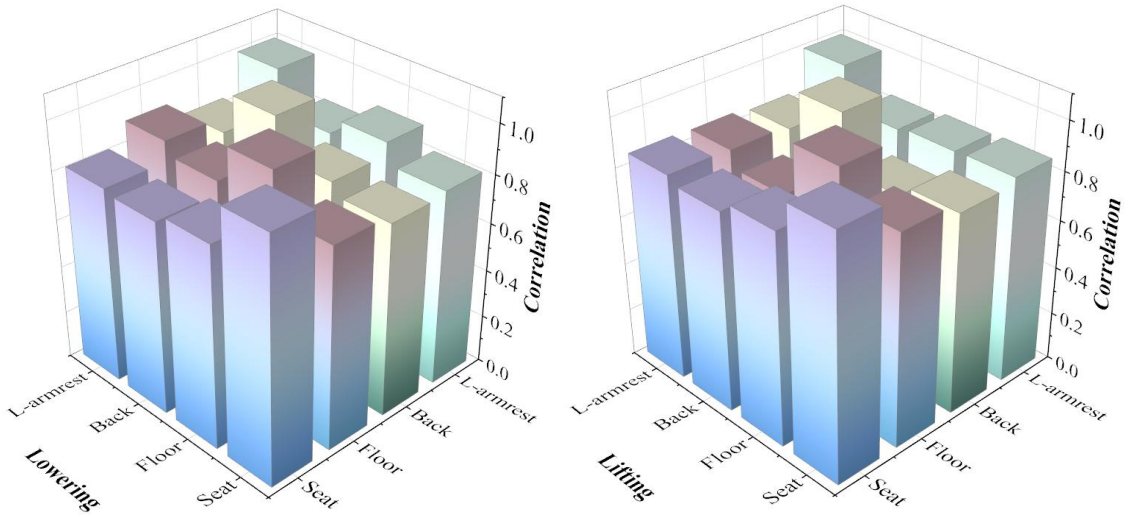

(a) **(b)**

Figure 8. The correlation of each measuring point in each working condition: **(a)** the correlation of subjective scores of each measuring point in the lowering condition; **(b)** the correlation of subjective scores of each measuring point in lifting condition.

4.2. Analysis of objective test results of vibration comfort

After the objective test is completed, the vibration signals of different measuring points are weighted by frequency and direction based on ISO-2631, and their RMS values are calculated for subsequent subjective and objective analysis and evaluation. ISO-2631 and related international standards mainly focus on conventional measuring points such as seat, floor and back, and do not specify the RMS calculation criteria for left armrest. In this study, the vibration signal of the left armrest is weighted by referring to the calculation criterion of the back, that is, the X, Y and Z directions are weighted by the frequency of W_c, W_d and W_d respectively.

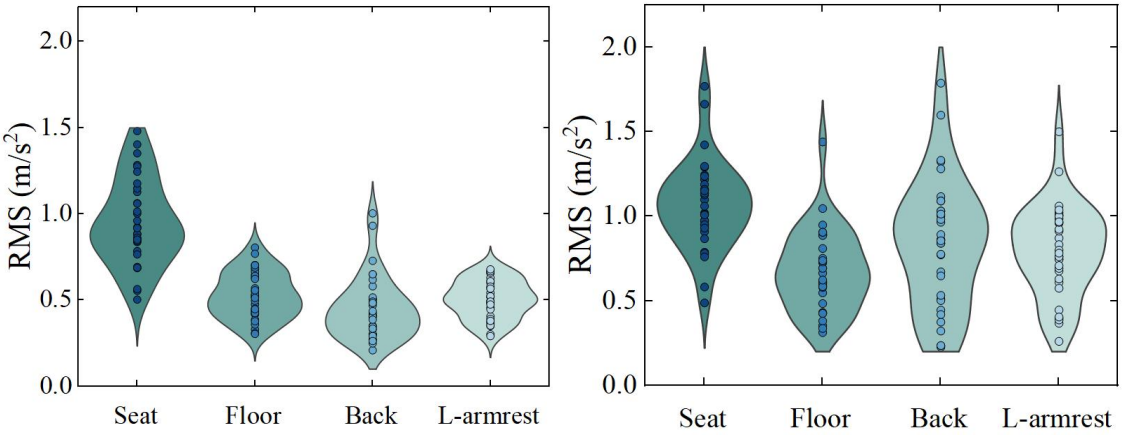

(a) **(b)**

Figure 9. RMS results of vibration measuring points under various working conditions: **(a)** RMS results of lowering conditions; **(b)** RMS results of lifting condition.

Figure 9 shows the RMS value distribution of the vibration signals of each measuring point after frequency weighting and direction weighting in the two working conditions of lifting and lowering. The analysis results show that in the lowering

condition, the vibration at the seat is the most significant, and its RMS value distribution is the most discrete and the mean value is the largest. The main reason is that during the lowering process, the boom and bucket fall back quickly with gravity, which makes it easier for vibration energy to be transmitted to the seat along the structural path. At the same time, due to individual differences such as different driver's body shape and sitting posture, the vibration response at the seat is further fluctuated, resulting in a more dispersed distribution of RMS values.

In contrast, in the lifting condition, the vibration at each measuring point is more severe, and the vibration at the back is the most significant. This may be due to the greater excitation intensity of the hydraulic system during the lifting process, resulting in a stronger instantaneous impact on the rear of the seat, so that the back produces a greater lateral torque around its shaft and enhances its vibration response. In addition, the vibration intensity at the left armrest is also obvious, which indirectly proves the rationality of increasing the measuring point of the left armrest. Overall, the vibration intensity and dispersion degree of the lifting condition are much larger than that of the lowering condition. This is because the hydraulic system needs to overcome the gravity during the lifting process to lift the boom and bucket together with the load, resulting in unstable excitation intensity.

4.3. Analysis of subjective and objective results

After completing the analysis of the subjective test results and objective test results of vibration comfort, to more intuitively show the subjective comfort performance of the loader in multiple vibration dimensions, this study uses a four-dimensional radar map to visualize the four vibration evaluation dimensions of the cab, as shown in **Figure 10**. Three representative subjective scoring samples are selected in the figure. Sample 1 shows that the overall vibration comfort is high, sample 2 reflects that the overall comfort is poor, and sample 3 shows that the comfort of a specific evaluation dimension is significantly low. The above three samples fully reflect a variety of typical perception scenarios of cab vibration comfort in loader operation.

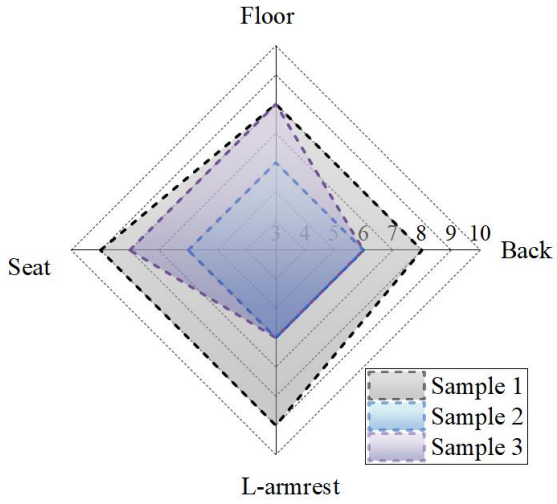

Figure 10. The subjective evaluation results of the four-dimensional vibration of the cab of three typical samples.

To describe the comprehensive comfort level of the cab from the overall perspective, this paper proposes to use the Overall Level (*OAL*) of the four-dimensional radar map as the characterization parameter of the comprehensive vibration comfort. The calculation method is shown in Equation (5):

$$OAL = \frac{1}{2}\sum_{i=1}^{4} x_i * x_{i+1} * sin(\frac{2\pi}{4}) \quad (5)$$

where, *OAL* represents the overall level of cab vibration comfort, x_i represents the subjective score of the *i* th evaluation dimension, and x_4=x_1, indicating that the radar chart is connected to form a closed space.

However, the *OAL* index can only reflect the overall level of the score, and it is difficult to describe the distribution differences between the evaluation dimensions. To further quantify the degree of balance and dispersion between the evaluation dimensions, this paper introduces Standard Deviation (*SD*) as an auxiliary indicator. Its calculation equation is shown in Equation (6):

$$SD = \frac{\sum_{i=1}^{4}(x_i - \bar{x})^2}{4} \times 100\% \quad (6)$$

where, *SD* is standard deviation, $\bar{x}$ is the average subjective score of the four dimensions of the evaluation sample.

The *OAL* and *SD* of the three typical evaluation samples are shown in **Table 3**. The analysis results show that the *OAL* values of sample 1 and sample 2 are 144.5 and 72, respectively, indicating that there is a significant difference between the two in the comprehensive comfort level of vibration. However, the *SD* values of the two are 25 % and 0 %, respectively, indicating that the distribution of subjective scores in each evaluation dimension is relatively balanced, and the difference between dimensions is small. In contrast, the *OAL* value of sample 3 was 98, and the *SD* value was 100 %. The results not only show that the comprehensive comfort level of vibration of sample 3 is low, but also the scores of each dimension are very different, reflecting that the sample has significant local discomfort, which is a typical case of poor comfort and uneven distribution of perception. The above results are consistent with the visual analysis in **Figure 10**, indicating that the comprehensive vibration comfort index *OAL* and the standard deviation *SD* can complement each other, which can more comprehensively and effectively describe the multi-dimensional perception characteristics of the subjective comfort of the cab vibration.

Table 3. Comprehensive comfort and standard deviation statistics of three typical samples.

Sample	*OAL*	*SD*
Sample 1	144.5	25%
Sample 2	72	0%
Sample 3	98	100%

5. Vibration comfort prediction model of loader

5.1. Construction of vibration comfort prediction model

In this chapter, an ACO-Transformer model is proposed for the multi-dimensional subjective and objective vibration data of the loader cab to achieve accurate prediction of the vibration comfort of the cab. The model aims to construct a nonlinear mapping relationship between the objective vibration indexes of the four measuring points of seat, floor, back and left armrest and the multi-dimensional subjective comfort score under lifting and falling conditions. The overall structure of the ACO-Transformer model is shown in **Figure 11**. The input of the model is the RMS values of four measuring points (seat, floor, back and left armrest) in X, Y and Z directions under each working condition, with a total of 12 input feature dimensions. The model output is the corresponding subjective scoring results of the above four measuring points.

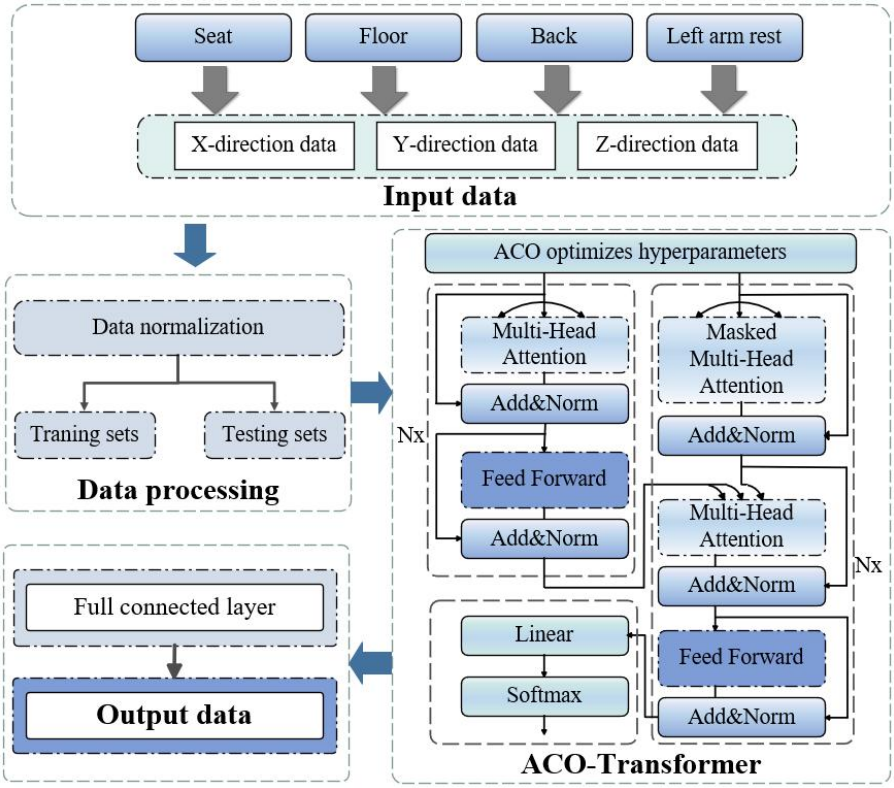

Figure 11. ACO-Transformer model building flow chart.

In this study, a total of 34 drivers' test data were collected. Since each driver was operated under two typical working conditions of lifting and falling, a total of 68 subjective and objective test samples were obtained. To improve the efficiency and stability of model training, the data set is first standardized. Then the sample set is divided into training set and test set according to the ratio of 8:2, in which the training set contains 54 sets of samples and the test set contains 14 sets of samples. Therefore, the input data dimension of the model training is 54 × 12, and the output data dimension is 54 × 4.

In addition, to reduce the fluctuation of the model caused by the contingency of

data set division and improve the stability and reliability of the prediction results. In this study, the model was trained and predicted 10 times independently. Each training uses a randomly divided data set, and finally the average of the 10 prediction results is used as the final prediction result of the model.

Table 4 shows the key parameter settings of the ACO-Transformer model. In terms of the structure of the model, the number of layers of the encoder and decoder is set to 6, the number of attention heads is set to 2, and the embedding dimension (Embedding dim) is set to 32 to ensure sufficient feature extraction and modeling capabilities. In terms of data input, considering that each sample contains 12-dimensional features, the total number of samples is 54, and the Batch Size is set to 16 to strike a balance between training efficiency and model stability. In terms of hyperparameter optimization, the maximum number of iterations (Num iter) of ACO algorithm is set to 10, the ant colony size (Num ants) is set to 12, and the pheromone volatilization coefficient (ρ) is set to 0.3, to ensure the effective exploration and convergence of hyperparameter space under reasonable calculation cost.

Table 4. ACO-Transformer model parameter table.

Parameter	Setting
Encoder dim	6
Decoder dim	4
Attention heads	2
Embedding dim	32
Batch size	16
Num iter	10
Num ants	12
ρ	0.3

5.2. Prediction and verification of vibration comfort model

To quantify the prediction error of the model and intuitively compare the performance of different models in the prediction of vibration comprehensive comfort, this study used Root Mean Square Error (RMSE) and Mean Absolute Percentage Error (MAPE) as the main evaluation indicators [53–55]. In addition, to further evaluate the fitting accuracy of the model in each evaluation dimension, this paper introduces the Cosine Similarity (*CS*) index to quantify the overall fitting difference between the model prediction result and the actual subjective score in each dimension. The larger the value, the more formal the prediction result and the real score shape of the model in each dimension. The calculation formula is shown in Equation (7):

$$CS = \frac{A \cdot B}{\|A\| \cdot \|B\|} \tag{7}$$

where, *CS* represents the shape similarity between the predicted value and the real value, *A* represents the predicted sample score, *B* represents the real sample score, $\|\cdot\|$ represents the model of the sample score.

In the 10 independent trainings of the ACO-Transformer model, the performance indicators of each prediction result are shown in **Table 5**. The results show that the average MAPE of the model in 10 predictions is 6.22 %, RMSE is 6.11, and *CS* is

0.966. This shows that the randomness of data set division has little effect on the prediction performance of the model. The ACO-Transformer model maintains high consistency and prediction accuracy in many experiments, which fully reflects the good stability and generalization ability of the model.

Table 5. ACO-Transformer model 10 independent training performance indicators of each prediction result.

Number	RMSE	MAPE	*CS*
1	6.05	6.28%	0.994
2	6.15	6.19%	0.995
3	6.18	6.32%	0.995
4	6.08	6.17%	0.996
5	6.10	6.20%	0.995
6	6.13	6.44%	0.994
7	6.07	6.06%	0.996
8	6.12	6.23%	0.995
9	6.11	6.21%	0.995
10	6.08	6.18%	0.996
Average	6.11	6.22%	0.995

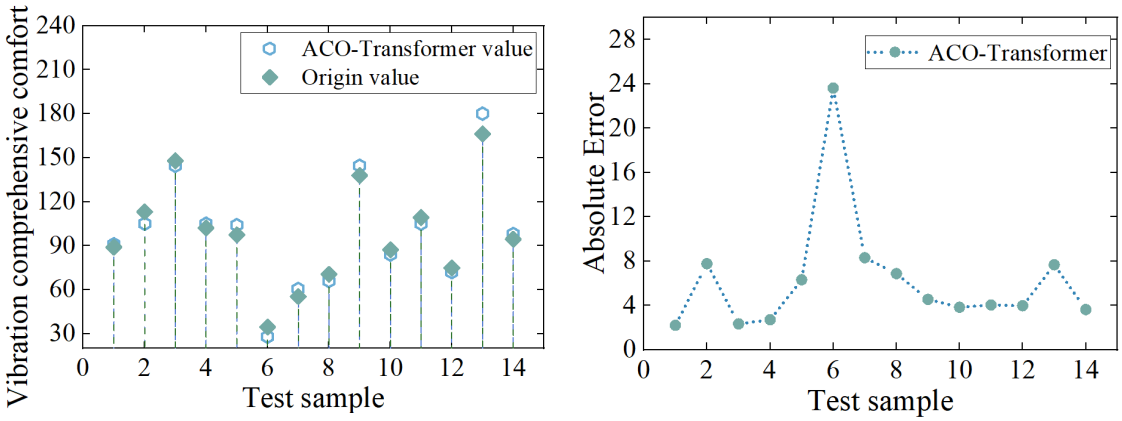

(a) **(b)**

Figure 12. Prediction results and errors of ACO-Transformer test set: **(a)** prediction results of vibration comprehensive comfort; **(b)** relative error of vibration comprehensive comfort prediction.

To intuitively show the prediction effect of the ACO-Transformer model on the test set, this paper selects the prediction results in the fifth training for visual presentation. The overall prediction performance of this experiment is close to the average level of 10 experiments, which is representative. As shown in **Figure 12**, the ACO-Transformer model can effectively capture the complex nonlinear mapping relationship between the objective vibration index and the driver's subjective score, and has strong prediction accuracy and fitting ability, which can accurately predict the multi-dimensional vibration comfort of the cab. In addition, by analyzing **Figure 12(a)** and **Figure 12(b)**, it can be found that the prediction error of the No.6 test sample is significantly higher than that of other samples. This is mainly because the No.6 sample is at an outlier in the sample distribution, and its feature distribution is quite different

from most samples, resulting in a decrease in the accuracy of the model when predicting the sample.

Subsequently, this paper visualizes and analyzes the vibration comfort prediction results of each evaluation dimension of the loader cab. Three representative typical samples in the test set are selected, and the radar chart of their actual subjective scores and model prediction results is drawn, as shown in **Figure 13**. **Table 6** shows the prediction error of the ACO-Transformer model in three typical samples. The results show that the ACO-Transformer model can accurately fit the subjective scoring curve of each sample. This verifies that the ACO-Transformer model can adapt to different comfort distributions. It also shows that it has good multi-objective modeling ability and can achieve stable and reliable prediction performance based on balancing multiple vibration dimensions.

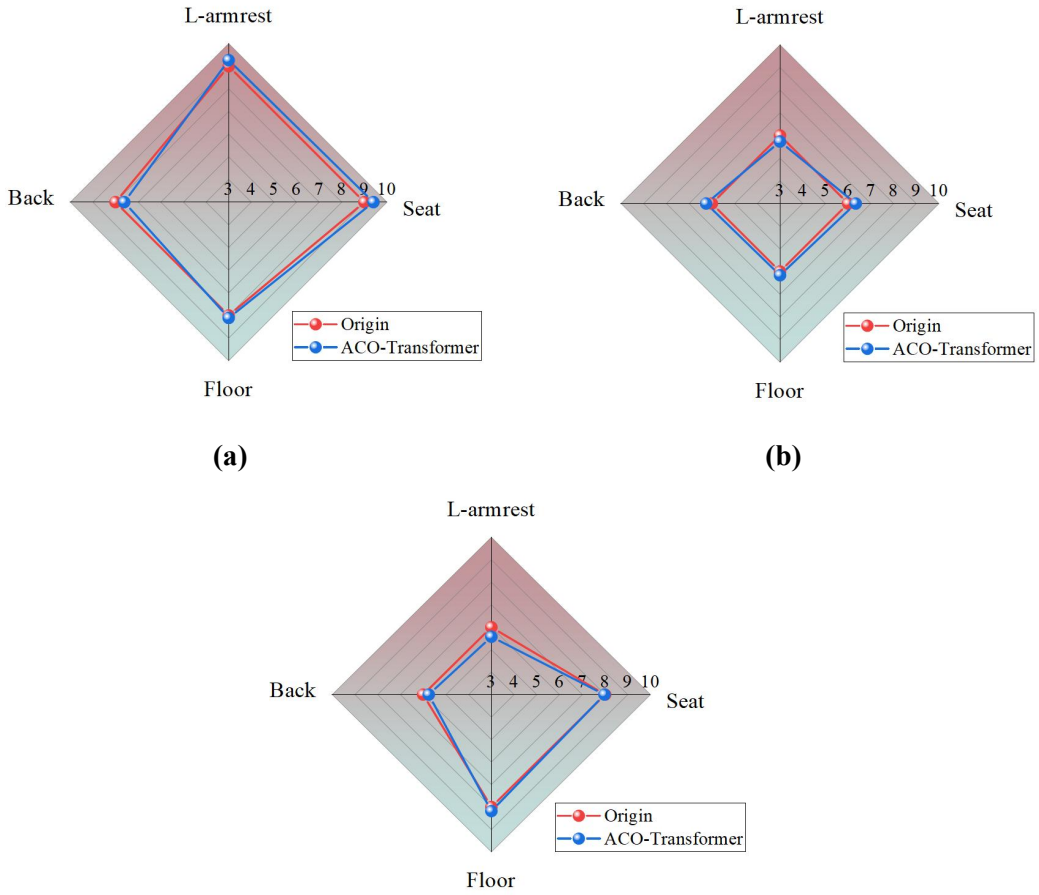

Figure 13. Vibration comprehensive comfort prediction radar chart: **(a)** samples with high overall comfort; **(b)** samples with low overall comfort; **(c)** samples with large differences in comfort perception in each dimension.

Table 6. The prediction error of ACO-Transformer on three typical samples.

Sample	RMSE	MAPE
The overall comfort is higher sample	3.36	2.32%
The overall comfort is lower sample	2.86	3.97%
Samples with large differences in comfort perception in each dimension	3.56	3.63%

To further verify the effectiveness of ACO-Transformer model in the prediction of comprehensive comfort of loader cab vibration, three models of Transformer, ACO-CNN and ACO-LSTM were introduced for comparative analysis. The structural design and parameter setting of the ACO-CNN and ACO-LSTM models are detailed in Appendix Figures S1 and S2 and Tables S2 and S3. To ensure the fairness of the comparison, the four models were trained and tested based on the same data set, and 10 independent training experiments were uniformly adopted. The average of the 10 prediction results of each model was used as the final output result. **Figure 14** shows the vibration comprehensive comfort prediction effect of the four models on the test set in the fifth training. The results show that the ACO-Transformer model has better prediction accuracy, robustness and robustness than other comparison models.

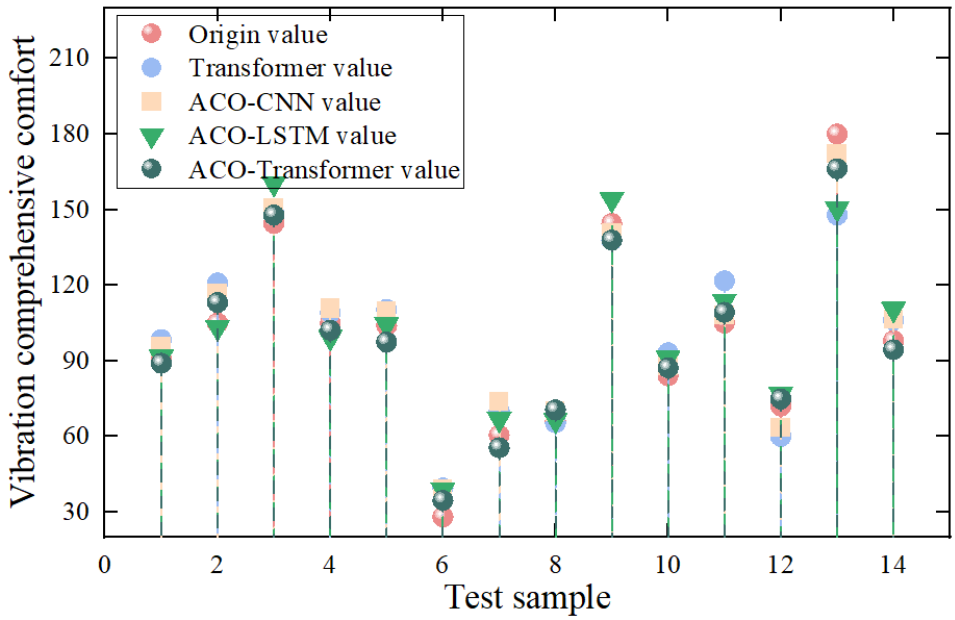

Figure 14. Comparison of prediction results of Transformer, ACO-CNN, ACO-LSTM and ACO-Transformer models.

To quantify the performance differences of each model in the vibration comfort prediction task, this paper summarizes the average evaluation indicators of the test set prediction results of the four models in 10 independent trainings in **Table 7**. The results show that the MAPE of ACO-Transformer, ACO-LSTM and ACO-CNN on the test set are 6.22%, 8.18% and 9.55% respectively, RMSE are 6.11, 11.07 and 10.63 respectively, and *CS* are 0.995, 0.979 and 0.981 respectively. The above results show that ACO-Transformer is compared with ACO-LSTM based on recurrent neural network and ACO-CNN based on convolutional neural network. It shows better prediction accuracy and fitting ability when dealing with multi-input and multi-output complex nonlinear subjective and objective mapping problems. It achieves the best results on all three indicators, showing stronger generalization ability and modeling stability. This is because the multi-head attention mechanism in the Transformer architecture has the global modeling ability of the input features, which can more effectively capture the interaction and potential coupling features between the vibration evaluation dimensions. In addition, the traditional Transformer model

performed worst among the four models, with MAPE, RMSE and *CS* of 11.07%, 12.72 and 0.966, respectively. By comparing with the results of ACO-Transformer, the effectiveness of ACO in model hyperparameter optimization is further verified. ACO can effectively improve the learning efficiency and adaptability of the model in high-dimensional space, to achieve more accurate and robust multi-objective prediction of the comprehensive comfort of cab vibration.

Table 7. The average index comparison of Transformer, ACO-CNN, ACO-LSTM and ACO-Transformer models on the test set is carried out.

Model	RMSE	MAPE	*CS*
Transformer	12.72	11.07%	0.966
ACO-CNN	10.63	9.55%	0.981
ACO-LSTM	11.07	8.18%	0.979
ACO-Transformer	6.11	6.22%	0.995

6. Conclusion

Based on the current lack of research on the evaluation method of vibration comfort of electric loader cab, this paper proposes a comprehensive evaluation and prediction method of vibration comfort analysis, and studies the comprehensive vibration comfort of electric loader cab, mainly including the following aspects:

Firstly, based on the driver's actual feelings and the transmission characteristics of the cab structure, an objective evaluation method of vibration comfort including four key positions of seat, floor, and left handrail is constructed in this study. Subsequently, a multi-dimensional subjective evaluation scale covering the above four measuring points is designed by combining the hierarchical division method and the semantic subdivision method to fully characterize the driver's subjective perception of the cab vibration comfort. Through the subjective and objective test of vibration comfort of electric loader, the subjective and objective data of 34 drivers were collected. On this basis, this study further proposes the vibration comprehensive comfort evaluation index *OAL* and *SD*, which are used to measure the overall comfort level of the cab and the balance of the scores of each dimension.

Secondly, the ACO-Transformer network model based on ant colony optimization algorithm is constructed by using 12 objective RMS indexes of the above four measuring points in X, Y and Z directions as model input, and compared with Transformer, ACO-LSTM and ACO-CNN models. The results show that ACO-Transformer performs best in terms of prediction accuracy and robustness. Its MAPE on the test set is 6.22 %, RMSE is 6.11, and *CS* is 0.995, which effectively verifies the applicability and superiority of the proposed model in the vibration comfort prediction task of the electric loader cab.

In addition, considering that the combination of multiple models can improve the accuracy and generalization of vibration comfort prediction, in future research, it is planned to further explore the performance of ensemble learning methods such as Bagging, Boosting, and Stacking applied to the vibration comfort prediction of the cab of electric loaders, and improve the accuracy and robustness of vibration comfort prediction. At the same time, to further optimize the model structure and training efficiency, subsequent research will also consider introducing feature selection or

dimensionality reduction techniques to achieve a better balance between model complexity and performance.

Author contributions: Conceptualization, RD and JZ; methodology, RD and HH; software, RD; validation, HH, WD and QS; investigation, WZ; writing—original draft preparation, RD and JZ; writing—review and editing, RD; visualization, HH; supervision, QS; funding acquisition, WZ. All authors have read and agreed to the published version of the manuscript.

Funding: This research was funded by China FAW Corporation Limited, grant number RBJ37-ZX.

Acknowledgments: The authors would like to acknowledge the support from the Institute of Energy and Power Research for the experimental research.

Availability of data and materials: The authors do not have permission to share the data.

Conflict of interest: The authors declare no conflict of interest.

References

1. Soresini F, Barri D, Ballo F, et al. Noise, vibration, and harshness countermeasures of permanent magnet synchronous motor with viscoelastic layer material. SAE International Journal of Vehicle Dynamics, Stability, and NVH. 2025; 9(4). doi: 10.4271/10-09-04-0031
2. Huang HB, Huang XR, Wu JH, et al. Novel method for identifying and diagnosing electric vehicle shock absorber squeak noise based on a DNN. Mechanical Systems and Signal Processing. 2019; 124: 439-458. doi: 10.1016/j.ymssp.2019.01.053
3. Tempone GP, de Carvalho Pinheiro H, Imberti G, et al. Control system for regenerative braking efficiency in electric vehicles with electro-actuated brakes. SAE International Journal of Vehicle Dynamics, Stability, and NVH. 2024; 8(2). doi: 10.4271/10-08-02-0015
4. Brozovsky J, Labonnote N, Vigren O. Digital technologies in architecture, engineering, and construction. Automation in Construction. 2024; 158: 105212. doi: 10.1016/j.autcon.2023.105212
5. Gao D, Zhou Z, Li P, et al. IncorporationNet: A novel bimodal EEG-EOG vigilance estimation method via time-frequency-space feature fusion network. Computer Methods in Biomechanics and Biomedical Engineering. 2025; 1-18. doi: 10.1080/10255842.2025.2515517
6. Gaspar J, Tefft B, Carney C, et al. The impact of self-initiated breaks during drowsy driving. SLEEP. 2025. doi: 10.1093/sleep/zsaf150
7. Wen Y, Wang B, Song Y, et al. Evaluation of vibration comfort and annoyance rate of an aircraft. Journal of Physics: Conference Series. 2025; 2977(1): 012036. doi: 10.1088/1742-6596/2977/1/012036
8. Huang HB, Wu JH, Huang XR, et al. A generalized inverse cascade method to identify and optimize vehicle interior noise sources. Journal of Sound and Vibration. 2020; 467: 115062. doi: 10.1016/j.jsv.2019.115062
9. Dai R, Zhao J, Zhao W, et al. Exploratory study on sound quality evaluation and prediction for engineering machinery cabins. Measurement. 2025; 253: 117684. doi: 10.1016/j.measurement.2025.117684
10. Kat CJ, Skrickij V, Shyrokau B, et al. Vibration-induced discomfort in vehicles: A comparative evaluation approach for enhancing comfort and ride quality. SAE International Journal of Vehicle Dynamics, Stability, and NVH. 2024; 8(2). doi: 10.4271/10-08-02-0009
11. Yang J, Chen Y, Xing S, et al. A comfort evaluation method based on an intelligent car cockpit. Human Factors and Ergonomics in Manufacturing & Service Industries. 2022; 33(1): 104-117. doi: 10.1002/hfm.20973
12. Peng C, Cheng S, Sun M, et al. Prediction of sound transmission loss of vehicle floor system based on 1D-Convolutional Neural Networks. Sound & Vibration. 2024; 58(1): 25-46. doi: 10.32604/sv.2024.046940
13. Suzuki K, Dang PT, Homma H, et al. Improved numerical estimation method for surface wave attenuation on metasurfaces. Advanced Theory and Simulations. 2024; 7(6). doi: 10.1002/adts.202301173

14. Iijima Y, Okumura Y, Yamasaki S, et al. Assessing the hierarchy of personal values among adolescents: A comparison of rating scale and paired comparison methods. Journal of Adolescence. 2020; 80(1): 53-59. doi: 10.1016/j.adolescence.2020.02.003
15. Huang H, Huang X, Ding W, et al. Uncertainty optimization of pure electric vehicle interior tire/road noise comfort based on data-driven. Mechanical Systems and Signal Processing. 2022; 165: 108300. doi: 10.1016/j.ymssp.2021.108300
16. Bouzir TAK, Berkouk D, Eisenman TS, et al. Soundscapes in Arab cities: A systematic review and research agenda. Sound & Vibration. 2024; 58(1): 1-24. doi: 10.32604/sv.2024.046723
17. Rainio O, Teuho J, Klén R. Evaluation metrics and statistical tests for machine learning. Scientific Reports. 2024; 14(1). doi: 10.1038/s41598-024-56706-x
18. Xiong JQ. Research on subjective rating attenuation analysis of automobile NVH characteristics. Procedia Computer Science. 2019; 154: 383-388. doi: 10.1016/j.procs.2019.06.055
19. Ao D, Wong PK, Huang W, et al. Analysis of co-relation between objective measurement and subjective assessment for dynamic comfort of vehicles. International Journal of Automotive Technology. 2020; 21(6): 1553-1567. doi: 10.1007/s12239-020-0146-0
20. Wu J, Zhang L, Meng D, et al. Evaluation of vibration comfort for vehicle seats with extensive backrest angles based on road tests. Journal of Mechanical Science and Technology. 2025; 39(5): 2587-2598. doi: 10.1007/s12206-025-0417-9
21. Hu Z. Construction and experimental study on subjective evaluation system of braking performance of new energy vehicle ABS system. IOP Conference Series: Materials Science and Engineering. 2019; 677(5): 052102. doi: 10.1088/1757-899x/677/5/052102
22. Zhan J, Zhu H, Duan C, et al. Modeling and subjective evaluation method of driveability for fuel cell vehicles. Energies. 2024; 17(7): 1620. doi: 10.3390/en17071620
23. Zhu B, Guo H, Zheng L, et al. A novel subjective evaluation method for the sound quality of high-speed train compartments. Journal of Vibration and Control. 2023; 30(11-12): 2325-2337. doi: 10.1177/10775463231184107
24. Tran T, Järvinen J. Understanding the concept of subjectivity in performance evaluation and its effects on perceived procedural justice across contexts. Accounting & Finance. 2022; 62(3): 4079-4108. doi: 10.1111/acfi.12916
25. Yang M, Dai P, Yin Y, et al. Predicting and optimizing pure electric vehicle road noise via a locality-sensitive hashing transformer and interval analysis. ISA Transactions. 2025; 157: 556-572. doi: 10.1016/j.isatra.2024.11.059
26. Huang H, Lim TC, Wu J, et al. Multitarget prediction and optimization of pure electric vehicle tire/road airborne noise sound quality based on a knowledge- and data-driven method. Mechanical Systems and Signal Processing. 2023; 197: 110361. doi: 10.1016/j.ymssp.2023.110361
27. Steinmetz MFA, Aschersleben J, Panagiotidou A. On-road measurements and modelling of disc brake temperatures and brake wear particle number emissions on a heavy-duty tractor trailer. Atmosphere. 2025; 16(5): 561. doi: 10.3390/atmos16050561
28. ISO, ISO. 2631-1: Mechanical vibration and shock-evaluation of human exposure to whole-body vibration-Part 1: General requirements. Geneva, Switzerland: ISO 42 1997: 43-4.
29. BSI, BS. 6841: 1987 Guide to measurement and evaluation of human exposure to whole-body mechanical vibration and repeated shock. BS.6841, BSI, 1987.
30. VDI, VDI. 2057: Human exposure to mechanical vibrations - Whole-body vibration. Düsseldorf: Verein Deutscher Ingenieure 2002.
31. Ciloglu H, Alziadeh M, Mohany A, et al. Assessment of the whole body vibration exposure and the dynamic seat comfort in passenger aircraft. International Journal of Industrial Ergonomics. 2015; 45: 116-123. doi: 10.1016/j.ergon.2014.12.011
32. Carletti E, Pedrielli F. Tri-axial evaluation of the vibration transmitted to the operators of crawler compact loaders. International Journal of Industrial Ergonomics. 2018; 68: 46-56. doi: 10.1016/j.ergon.2018.06.007
33. Zhao X, Kremb M, Schindler C. Assessment of wheel loader vibration on the riding comfort according to ISO standards. Vehicle System Dynamics. 2013; 51(10): 1548-1567. doi: 10.1080/00423114.2013.814798
34. Cheng L, Wen H, Ni X, et al. Optimization study on the comfort of human-seat coupling system in the cab of construction machinery. Machines. 2022; 11(1): 30. doi: 10.3390/machines11010030
35. Zhao Y, Liu J, Ma L, et al. Test and evaluation of driving comfort of rice combine harvester. PLOS ONE. 2023; 18(6): e0287138. doi: 10.1371/journal.pone.0287138

36. Guastadisegni G, De Pinto S, Cancelli D, et al. Ride analysis tools for passenger cars: objective and subjective evaluation techniques and correlation processes—A review. Vehicle System Dynamics. 2023; 62(7): 1876-1902. doi: 10.1080/00423114.2023.2259024
37. Paul P, Banerjee S, Nandi A, et al. A multilayer deep neural network framework for hemodynamic assessment of cognitive load management during problem-solving tasks. Cognitive Neurodynamics. 2025; 19: 104. doi: 10.1007/s11571-025-10292-4
38. Huang X, Huang H, Wu J, et al. Sound quality prediction and improving of vehicle interior noise based on deep convolutional neural networks. Expert Systems with Applications. 2020; 160: 113657. doi: 10.1016/j.eswa.2020.113657
39. Huang HB, Li RX, Yang ML, et al. Evaluation of vehicle interior sound quality using a continuous restricted Boltzmann machine-based DBN. Mechanical Systems and Signal Processing. 2017; 84: 245-267. doi: 10.1016/j.ymssp.2016.07.014
40. Marotta R, Strano S, Terzo M, et al. Multi-output physically analyzed neural network for the prediction of tire–road interaction forces. SAE International Journal of Vehicle Dynamics, Stability, and NVH. 2024; 8(2). doi: 10.4271/10-08-02-0016
41. Huang H, Huang X, Ding W, et al. Vehicle vibro-acoustical comfort optimization using a multi-objective interval analysis method. Expert Systems with Applications. 2023; 213: 119001. doi: 10.1016/j.eswa.2022.119001
42. Du X, Sun C, Zheng Y, et al. Evaluation of vehicle vibration comfort using deep learning. Measurement. 2021; 173: 108634. doi: 10.1016/j.measurement.2020.108634
43. Li H, Chen A, Yi J, et al. Environmental sound classification based on CAR-Transformer neural network model. Circuits, Systems, and Signal Processing. 2023; 42(9): 5289-5312. doi: 10.1007/s00034-023-02339-w
44. Yang M, Song M, Guo Y, et al. Prediction of shield tunneling-induced ground settlement using LSTM architecture enhanced by multi-head self-attention mechanism. Tunnelling and Underground Space Technology. 2025; 161: 106536. doi: 10.1016/j.tust.2025.106536
45. Blum C. Ant colony optimization: A bibliometric review. Physics of Life Reviews. 2024; 51: 87-95. doi: 10.1016/j.plrev.2024.09.014
46. Zhu H, Zhao J, Wang Y, et al. Improving of pure electric vehicle sound and vibration comfort using a multi-task learning with task-dependent weighting method. Measurement. 2024; 233: 114752. doi: 10.1016/j.measurement.2024.114752
47. Skackauskas J, Kalganova T, Dear I, et al. Dynamic impact for ant colony optimization algorithm. Swarm and Evolutionary Computation. 2022; 69: 100993. doi: 10.1016/j.swevo.2021.100993
48. Zhou X, Ma H, Gu J, et al. Parameter adaptation-based ant colony optimization with dynamic hybrid mechanism. Engineering Applications of Artificial Intelligence. 2022; 114: 105139. doi: 10.1016/j.engappai.2022.105139
49. Pang J, Mao T, Jia W, et al. Prediction and analysis of vehicle interior road noise based on mechanism and data series modeling. Sound & Vibration. 2024; 58(1): 59-80. doi: 10.32604/sv.2024.046247
50. Huang H, Wang Y, Wu J, et al. Prediction and optimization of pure electric vehicle tire/road structure-borne noise based on knowledge graph and multi-task ResNet. Expert Systems with Applications. 2024; 255: 124536. doi: 10.1016/j.eswa.2024.124536
51. Moore BCJ, Lowe DA, Cox G. Guidelines for diagnosing and quantifying noise-induced hearing loss. Trends in Hearing. 2022; 26. doi: 10.1177/23312165221093156
52. Tang SJ, Zhang KF, Dong R, et al. The effect of vertical whole-body vibration with different frequencies on the dynamic biomechanics of sitting human waist. Proceedings of the Institution of Mechanical Engineers, Part C: Journal of Mechanical Engineering Science. 2024; 239(6): 1815-1825. doi: 10.1177/09544062241297126
53. Gautam A, He Y, Lin X. An overview of motion-planning algorithms for autonomous ground vehicles with various applications. SAE International Journal of Vehicle Dynamics, Stability, and NVH. 2024; 8(2). doi: 10.4271/10-08-02-0011
54. He Z, Guo H, Liu H, et al. A sound quality evaluation method for vehicle interior noise based on auditory loudness model. Sound & Vibration. 2024; 58(1): 47-58. doi: 10.32604/sv.2024.045470
55. Ma Y, Dai R, Liu T, et al. Physics-informed GRU model for vehicle road noise prediction: Integrating transfer path analysis and hybrid data. Sound & Vibration. 2025; 59(3): 3143. doi: 10.59400/sv3143

Appendix

Table A1. Statistical table of subjective score correlation of each measuring point.

		Seat	Floor	Back	L-armrest
Lowering	Seat	1	0.84	0.80	0.81
	Floor	0.84	1	0.85	0.90
	Back	0.80	0.85	1	0.83
	L-armrest	0.81	0.90	0.83	1
Lifting	Seat	1	0.87	0.83	0.86
	Floor	0.87	1	0.78	0.85
	Back	0.83	0.78	1	0.84
	L-armrest	0.86	0.85	0.84	1

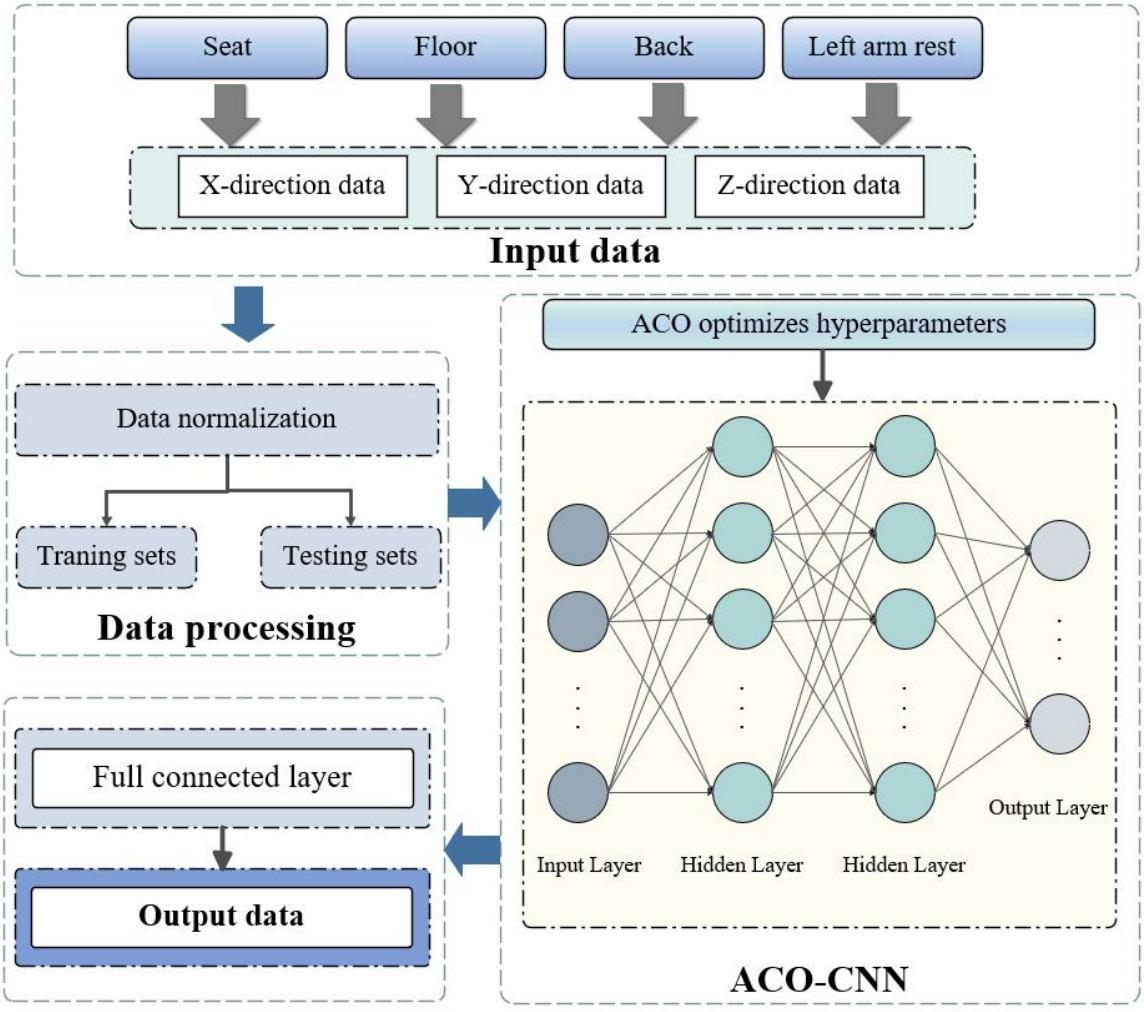

Figure A1. ACO-CNN model building flow chart.

The overall structure of the ACO-CNN model is shown in **Figure A1**. The vibration RMS values of four key measuring points (seat, floor, back and left armrest) in X, Y and Z directions under each group of working conditions are input into the model, a total of 12 input feature dimensions, the output of the model is the subjective scoring results of the corresponding four measuring points. **Table A2** lists the main parameter settings of the ACO-CNN model. In

terms of model structure, the number of convolution layers (Num conv layers) is set to 2, the size of convolution kernel (Kernel size) is set to 3, and the number of channels (Channels) of each convolution layer is set to 16 and 32 respectively. The Batch Size is set to 8 to achieve a balance between model training efficiency and stability. In terms of hyperparameter optimization, the maximum number of iterations (Num iter) of the ACO algorithm is set to 20, the ant colony size (Num ants) is 22, and the pheromone volatilization coefficient (ρ) is set to 0.3, to achieve full search and effective convergence of the hyperparameter space under the premise of reasonable computational overhead.

Table A2. ACO-CNN model parameter table.

Parameter	Setting
Num conv layers	2
Kernel size	3
channels	[16,32]
Batch size	8
Num iter	20
Num ants	22
ρ	0.3

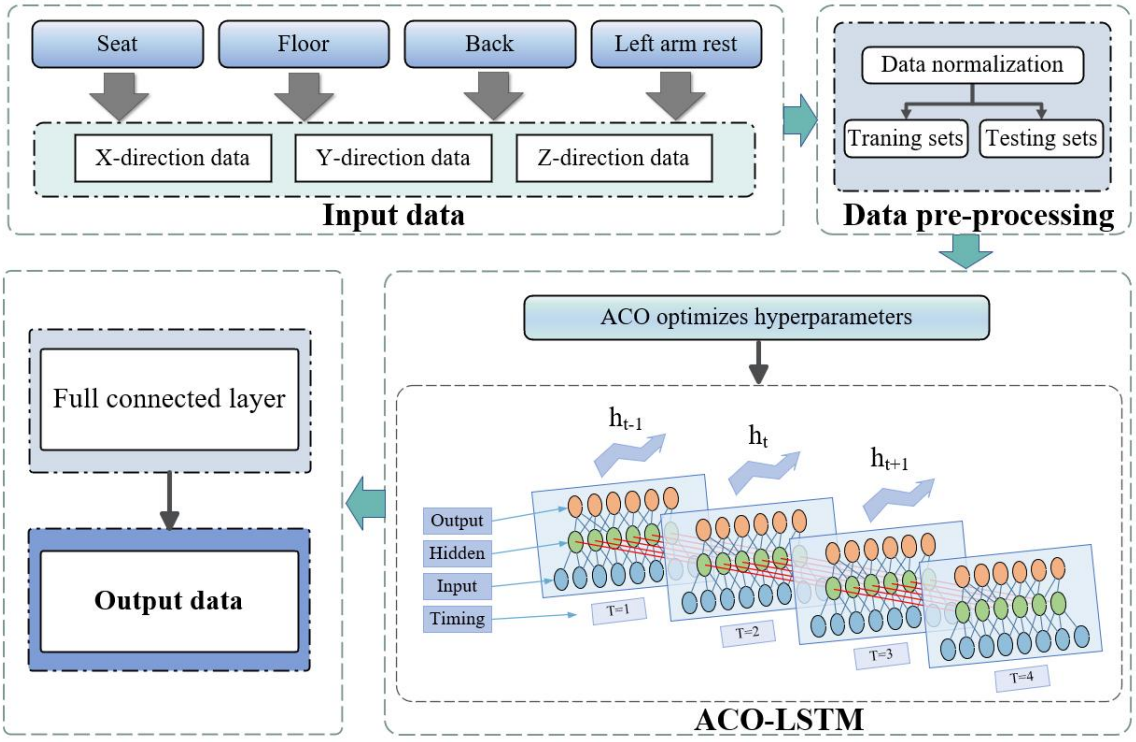

Figure A2. ACO-LSTM model building flow chart.

Figure A2 shows the overall architecture of the ACO-LSTM model. The input of the model consists of the RMS values of the four measurement points (seat, floor, back, left armrest) in the X, Y, and Z directions under each working condition, with a total of 12 feature dimensions. These features can fully reflect the characteristics of cab vibration in different positions and directions. The model output is the subjective score of the four measurement points, which directly corresponds to the driver's comfort perception at each contact point. **Table A3** lists the main parameter settings of the ACO-LSTM model. ACO-LSTM adopts a network architecture with two layers of LSTM units stacked, each layer containing 64 hidden neurons. The batch size in the training phase is set to 8, so that the model can maintain high learning efficiency and avoid overfitting risks. Through this structure, the network can effectively learn the complex

relationship between vibration characteristics and scores under limited sample conditions. In the hyperparameter search process, the ACO algorithm is used to dynamically adjust the key parameter combination. In the optimization strategy, the maximum number of iterations (Num iter) is set to 30, the ant colony size (Num ants) is 20, and the pheromone volatility coefficient (ρ) is taken as 0.3. Such a configuration ensures a balance between sufficient exploration of the search space and pheromone convergence, thereby improving the stability of model training and prediction performance.

Table A3. ACO-CNN model parameter table.

Parameter	Setting
Num layers	2
Hidden size	64
Batch size	8
Num iter	30
Num ants	20
ρ	0.3